Pharm Res (2015) 32:640–653
DOI 10.1007/s11095-014-1492-2

RESEARCH PAPER

Pharmacokinetic and Pharmacodynamic Relationship of AMG 811, An Anti-IFN-γ IgG_1 Monoclonal Antibody, in Patients with Systemic Lupus Erythematosus

Ping Chen • Thuy Vu • Adimoolam Narayanan • Winnie Sohn • Jin Wang • Michael Boedigheimer • Andrew A. Welcher • Barbara Sullivan • David A. Martin • Juan Jose Perez Ruixo • Peiming Ma

Received: 30 January 2014 / Accepted: 15 August 2014 / Published online: 12 September 2014

ABSTRACT

Purpose To investigate the relationships between AMG 811 exposure, concentration changes in serum IFN-γ, and IFN-γ-induced protein 10 (CXCL10), and to identify important contributions of baseline covariates to these relationships.

Methods A mechanism based pharmacokinetic (PK)-pharmacodynamic (PD) model was developed. A target mediated disposition model was used to describe AMG 811 and target IFN-γ interaction. CXCL10 was predicted to be driven by estimated free IFN-γ levels.

Results For an average systemic lupus erythematosus (SLE) subject, the linear clearance (CL) of AMG 811 was 0.176 L/day, and the central (V_c) and peripheral (V_p) volumes of distribution were 1.48 and 2.12 L, respectively. Body weight was found to correlate with CL, V_c, V_p, and inter compartment clearance (Q); and age was found to correlate with V_c. The relationship between estimated free serum IFN-γ concentration levels and serum CXCL10 in logarithmic scales was best described by a linear model with slope and intercept estimated to be 0.197 and -0.3, respectively.

Conclusions The largest observed reduction of serum CXCL10 concentration was achieved at the highest AMG 811 dose tested (180 mg SC). This model enables simulations of AMG 811 PK-PD profiles under various dosing regimens to support future clinical studies.

KEY WORDS AMG 811 · Lupus · PK/PD modeling · IFN-γ · CXCL10

INTRODUCTION

IFN-γ is a major pro-inflammatory cytokine, that modulates the function of several important immune system cells, including B and T cells, and plays a crucial role in the differentiation and maturation of T cells in the T helper type 1 lineage (Th 1). IFN-γ also affects isotype switching in B cells, resulting in an increased production of antibody isotypes, that further contribute to pro-inflammatory processes [1,2]. In addition, IFN-γ activates macrophages and regulates chemokine synthesis such as CXCL10. These effects exhibit significant impact on activation of inflammatory cell populations [3].

There has been an increasing recognition of the pathologic potential of IFN-γ in human autoimmune disorders, including systemic lupus erythematosus (SLE) and lupus nephritis [4]. In preclinical studies, several lupus models have shown the beneficial effects of blocking IFN-γ [4,5]. Clinical studies have also linked IFN-γ with human SLE and lupus nephritis [6,7]. In addition, there is evidence that IFN-γ, or molecules whose expression is up-regulated by IFN-γ, such that CXCL10, are present at increased levels in SLE patients, particularly those with lupus nephritis [8–13]. More specifically, CXCL10 has been shown to be a major contributor to the overall association and an independent predictor of future disease flare in SLE [14]. Therefore, these studies collectively suggested that blocking IFN-γ may improve disease outcomes in SLE subjects and, consequently, the AMG 811 monoclonal antibody is being developed to target IFN-γ in order to test this hypothesis.

AMG 811 is a human antibody of IgG_1 isotype, expressed in Chinese hamster ovarian cells, that binds with high affinity

P. Chen • T. Vu • A. Narayanan • W. Sohn • J. Wang • J. J. P. Ruixo • P. Ma
Pharmacokinetics and Drug Metabolism, Thousand Oaks California, USA

M. Boedigheimer • A. A. Welcher • B. Sullivan
Medical Sciences, Amgen Inc, One Amgen Center Dr, 91320 Thousand Oaks California, USA

D. A. Martin
Medical Sciences, Amgen Inc, 1201 Amgen Court West, 98119 Seattle Washington, USA

P. Chen (✉)
Amgen Inc., MS 28-3-B, One Amgen Center Dr, 91320 Thousand Oaks California, USA
e-mail: pingc@amgen.com

to human IFN-γ (K_D=5 pM using kinetic exclusion assay technology KinExA® 3000, Sapidyne Instruments, Inc. Boise, ID). Preclinical studies performed using cell lines and whole blood from humans and chimpanzees showed that AMG 811 binds IFN-γ and blocks interaction with its receptor (data not shown). Based on these preclinical findings, AMG 811 has the potential of becoming an important therapeutic agent for treating SLE and other inflammatory diseases and is currently in clinical development. In phase 1 studies, the safety, tolerability, PK and PD of AMG 811 were evaluated following single or multiple doses given by IV or SC injection in SLE patients [15]. Non-compartmental analysis (NCA) suggested that AMG 811 was slowly absorbed after SC administration across the dose range evaluated, with median t_{max} between 4 and 14 days. For the SC doses, AMG 811 exposure (based on C_{max} and AUC) increased approximately dose-proportionally from 2 to 180 mg. Thus, AMG 811 exhibited linear PK properties, with a mean terminal half-life ($t_{1/2,z}$) that ranged from 12 to 21 days after IV and SC dosing [15]. Another anti-IFN-γ monoclonal antibody, fontolizumab, has reported a terminal half-life of 18 days, which is consistent with AMG 811 of the same isotype [16].

For the purpose of better predicting exposure and response in SLE patients and selecting doses in future clinical trials, a population PK-PD modeling analysis was used to elucidate the relationship of serum AMG 811 exposure with serum IFN-γ and CXCL10 levels, and to identify sources of both inter- and intra-subject PK-PD variability. In this manuscript we present the results of this PK-PD modeling analysis.

MATERIALS AND METHODS

Data and Study Design

Serum free AMG 811, serum total IFN-γ concentration (e.g. free + bound IFN-γ) and serum CXCL10 concentration data from two Amgen-sponsored phase 1 studies were used in this analysis; the 20060203 single-ascending dose study and the 20070283 (NCT00818948) multiple-ascending dose study. Both studies were randomized, double-blind, placebo-controlled studies in SLE patients. The purpose of these studies is to evaluate the safety, tolerability and pharmacokinetics of single dose and multiple dose of AMG 811. In these studies, single doses (20060203 study, 26 subjects in total) of 0, 2, 6, 20, 60 and 180 mg administered by SC route, 60 mg administered by IV route, and multiple SC doses (20070283 study, 28 subjects in total) of 0, 6, 20 and 60 mg administered monthly (QM) for a total of three doses were evaluated. In the single-dose study, intensive PK and serum total IFN-γ samples were collected from all subjects at 0 (predose), at 6 hours on day 1, and on days 2, 3, 5, 8, 15, 22, 29, 43, 56, 84, 112, 140, 168, and 196 post dose. Extra serum total IFN-γ samples were collected at 0.5 and 1 hour on day 1. Serum CXCL10 samples were collected at 0 (predose), post-dose on days 1, 8, 15 and at the end of study. In the multiple-dose study, PK and serum total IFN-γ samples were collected from all subjects at 0 hours (predose), at 6 hours on day 1, and on days 2, 5, 8, 15, 22, 29, 43; and at 0 hours (predose) and 6 hours on day 57, and on days 64, 71, 78, 85, 113, 141, 169 and the end of study. Serum CXCL10 samples were collected on day -1 (baseline), on days 1, 3, 8, 15 and at 0 (predose) on days 29, 57, 85, and 113 and at the end of study. All subjects signed informed consent, and were randomized to receive AMG 811 or placebo in a 3 to 1 ratio in each dose group. Patient baseline demographics from the two studies is shown in Table I.

AMG 811, TOTAL IFN-Γ AND CXCL10 ASSAYS

Serum AMG 811 and serum total IFN-γ concentrations were measured using sandwich immunoassays developed and validated at Amgen Inc., Thousand Oaks, CA. A mouse anti-AMG 811 monoclonal antibody (Amgen Inc.) was used as a capture reagent for the AMG 811 assay. Study serum samples were added to the coated plates after blocking nonspecific binding. Biotin conjugated rabbit anti-AMG 811 polyclonal antibodies (Amgen Inc.) were used as the detection reagent. After the incubation with streptavidin-HRP (KPL Inc., MD), the colorimetric determination of the horseradish peroxidase reaction with the tetramethylbenzidine peroxide substrate solution (KPL Inc., MD) was measured by optical density at 450 with reference to 650 nm. The serum sample concentrations were quantified by interpolation from a standard curve run in parallel on each micro-titer plate using a four-parameter logistic (auto-estimate) regression model with a weighting factor that was the reciprocal of the absorbance. The lower limit of quantification (LLOQ) of the assay was 15.2 ng/mL. The inter-assay coefficient of variation for standards (STD) and Quality Control samples (QC) ranged from 2% to 4% and 6% to 7%, respectively; the inter-assay accuracy for STDs and QCs ranged from −2% to 2% and −7% to 0%, respectively; and the total error for QCs ranged from 6% to 13%.

Recombinant human IFN-γ (Amgen Inc.) was used as calibration standards for the total IFN-γ assay. The study serum samples, along with STDs and QCs, were incubated with approximately 25 ug/mL of AMG 811 at 37°C to form

Table I Summary of subject baseline demographics used in PK-PD analysis

Demographic characteristics		20060203 ($n=26$)	20070283 ($n=28$)	Total ($n=54$)
Sex	Male (%)	2 (8%)	1 (4%)	3 (6%)
	Female (%)	24 (92%)	27 (96%)	51 (94%)
Race	Caucasian (%)	16 (62%)	17 (61%)	33 (61%)
	African American (%)	4 (15%)	5 (18%)	9 (17%)
	Hispanic (%)	5 (19%)	5 (18%)	10 (18%)
	Asian (%)	1 (4%)	0	1 (2%)
	Others (%)	0	1 (3%)	1 (2%)
Age (yr)[a]		43.6 (11.9)	40.5 (14)	45 (13)
		45.5 [21–67]	40.5 [20–68]	41.5 [20–68]
Weight (kg)[a]		74.9 (17.1)	75.4 (18.1)	75.1 (17.5)
		69.8 [47.7-105]	69.1 [50.8-115.4]	69.3 [47.7-115.4]
Baseline CXCL10 (nM)[a]		0.0537 (0.096)	0.021 (0.012)	0.0378 (0.07)
		0.0189 [0.00735-0.456]	0.0161 [0.011-0.058]	0.0171 [0.00735-0.456]

[a] Data expressed as mean (SD) median [range]; Baseline total IFN-γ level is not detected in most subjects

IFNγ-AMG 811 complex prior to being added to a plate that was coated with a mouse anti-IFN-γ monoclonal antibody (Hycult Biotechnology, Uden, Netherlands). The Biotin conjugated rabbit anti-AMG 811 polyclonal antibodies (Amgen Inc.) were used as detection reagent. After the incubation with streptavidin-HRP (KPL Inc., MD), the colorimetric determination of the horseradish peroxidase reaction with the tetramethylbenzidine peroxide substrate solution (KPL Inc., MD) was measured by optical density at 450 with reference to 650 nm. The serum sample concentrations were quantified by interpolation from a standard curve run in parallel on each micro-titer plate using a four-parameter logistic (auto-estimate) regression model with a weighting factor that was the reciprocal of the absorbance. The LLOQ of the assay was 50 pg/mL. The inter-assay coefficient of variation for STDs and QCs ranged from 1% to 7% and 4% to 6%, respectively; the inter-assay accuracy for STDs and QCs ranged from −3% to 6% and −4% to 2%, respectively; and the total error for QCs ranged from 7% to 8%. The *in-vitro* binding affinity of AMG 811 to human IFN-γ was evaluated using kinetic exclusion assay technology (KinExA® 3000, Sapidyne Instruments, Inc. Boise, ID). Samples were processed according to manufacturer's instructions.

Serum CXCL10 concentration was determined with a commercially available ELISA according to the manufacturer's instructions (R&D Systems, Minneapolis, MN). Serum samples were analyzed in triplicate and levels were quantified by interpolation from a standard curve run in parallel on each micro-titer plate. The LLOQ of the assay was 40 pg/mL. The intra-assay and inter-assay coefficient of variation ranged from 3.0% to 4.6% and 5.2% to 8.8%, respectively.

PK-PD ANALYSIS

Structural Model Development

The structural PK-PD model of AMG 811 is shown in Fig. 1 where a target-mediated disposition model (TMD) was used to describe the interaction between serum AMG 811 and serum total IFN-γ, and serum CXCL10 concentration change was driven by estimated free IFN-γ. SC dose was administed into a depot compartment via a zero-order kinetics and the duration (D1) of this process was estimated. The absorption of AMG 811 from the depot to the central compartment was represented by the first-order absorption rate constant (k_a). Absolute bioavailability (F) was estimated by simultaneously analyzing SC and IV PK data. Following IV or SC absorption, free AMG 811 was distributed into a central compartment with a volume of distribution of V_c and further distributed from a central compartment to a peripheral compartment with a volume of distribution of V_p to account for nonspecific drug binding. The elimination of free AMG 811 (described below) was characterized by a linear pathway via a first-order elimination rate constant (k_{el}), or by binding to its target (free IFN-γ). The binding of free AMG 811 with free IFN-γ was considered reversible with association and dissociation rate constants k_{on} and k_{off}, respectively, and the AMG 811- IFN-γ complex (RC) is assumed to be cleared with an elimination rate constant (k_{met}). The production of IFN-γ was assumed to follow zero-order kinetics characterized by synthesis rate k_{syn}, and the degradation followed a first-order process characterized by an elimination rate constant k_{deg}. As the general TMD model [17] resulted in over-parameterization and model instability given the current PK-PD information available, a TMD model with quasi-steady-state (Q_{ss}) approximation [18] was used in analyzing the AMG 811 and IFN-γ data. A Q_{ss} constant K_{ss} was

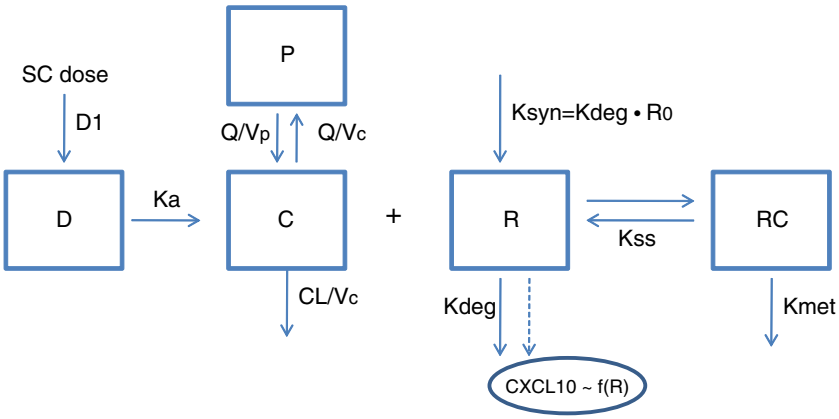

Fig. 1 Schematic representation of PK/PD model of AMG 811, total IFN-γ and CXCL10. D, C and P represent the depot, central and peripheral compartments, respectively. Subcutaneous (SC) dose is administered into depot compartment via a zero order kinetics (D1). The absorption of AMG 811 is represented by the first order absorption rate constant (k_a). Distribution from central compartment (V_c) to peripheral (V_p) compartment is linear with inter-compartment clearance Q. Drug elimination from central compartment is characterized using linear clearance (CL). R and RC represent free IFN-γ and AMG 811- IFN-γ complex compartments, respectively. K_{syn} and K_{deg} represent free IFN-γ production and degradation rate constant, respectively. The AMG 811-IFN-γ binding affinity is estimated as steady state constant K_{ss}. The elimination of drug-target complex is described using K_{met}. CXCL10 represents CXCL10 compartment and CXCL10 concentration change is driven by free IFN-γ.

defined in equation (1). The free AMG 811 concentration (C) was approximated through the total AMG811 (C_{tot}) and total IFN-γ concentrations (R_{tot}). The initial differential equations used for the PK-PD model are listed below:

$$k_{on}\cdot C\cdot R-(k_{met}+k_{off})\cdot RC=0\Rightarrow K_{ss}=\frac{C\cdot R}{RC}=\frac{(k_{off}+k_{met})}{k_{on}} \quad (1)$$

$$C=0.5\cdot\left[(C_{tot}-R_{tot}-K_{ss})+\sqrt{(C_{tot}-R_{tot}-K_{ss})^2+4K_{ss}\cdot C_{tot}}\right] \quad (2)$$

$$\frac{dA_d}{dt}=-k_a\cdot A_d \quad (3)$$

$$\frac{dA_{tot}}{dt}=k_a\cdot A_d+k_{pc}\cdot A_p-(k_{cp}+k_{el})\cdot C\cdot V_c-\frac{R_{tot}\cdot k_{met}\cdot C\cdot V_c}{(K_{ss}+C)} \quad (4)$$

$$\frac{dA_p}{dt}=k_{cp}\cdot C\cdot V_c-k_{pc}\cdot A_p \quad (5)$$

$$\frac{dR_{tot}}{dt}=k_{syn}-k_{deg}\cdot R_{tot}-\frac{(k_{met}-k_{deg})\cdot R_{tot}\cdot C}{(K_{ss}+C)} \quad (6)$$

Where C, R, and RC are the concentrations of free AMG 811 in the central compartment, free IFN-γ, and AMG 811-IFN-γ complex, respectively. A_d and A_p are the amount of free AMG811 in the depot, and peripheral compartments, respectively. A_{tot} is the amount of total AMG811 in the central compartment. V_c and V_p are the volumes of distribution in the central and peripheral compartments, respectively. C_{tot} is the total AMG811 concentration (i.e., C + RC). R_{tot} is the total IFN-γ concentration (i.e., R + RC). k_a, k_{el}, k_{cp} and k_{pc} are the absorption, elimination, central to peripheral, and peripheral to central rate constants, respectively. k_{on} and k_{off} are the AMG 811 with IFN-γ association and dissociation rate constants, respectively. k_{syn} and k_{deg} are the free IFN-γ production and degradation rate constants, respectively. Prior to drug treatment, IFN-γ was considered to be at steady state. Thus, k_{syn} = k_{deg} • baseline IFN-γ. k_{met} is the elimination rate constant of AMG 811- IFN-γ complex. K_{ss} is the Q_{SS} constant.

Since the free IFN-γ is negligible compared with the free drug concentration as evidenced by the observation that at day 90, the ratio of total IFN-γ and free AMG 811 are less than 1% (data not shown), total drug concentration (C_{tot}) is approximately equal to free drug concentration (C) in the central compartment. The equations (2) and (4) above could be simplified as shown below:

$$C=\frac{A_{tot}}{V_c} \quad (7)$$

$$\frac{dA_{tot}}{dt}=k_a\cdot A_d+k_{pc}\cdot A_p-(k_{cp}+k_{el})\cdot C\cdot V_c \quad (8)$$

During initial model development, this model was simultaneously fitted to the individual AMG 811 and total IFN-γ concentrations. The free IFN-γ was derived from the model using the following equation (9):

$$R = R_{tot} - RC = \frac{R_{tot} \cdot K_{ss}}{K_{ss} + C} \quad (9)$$

An exploratory graphical analysis (Fig. 2) of log transformed predicted free IFN-γ *vs* log transformed observed CXCL10 concentration suggested a clear linear relationship which is consistent with the underlying mechanism that CXCL10 expression is induced by free IFN-γ. Thus, a linear model was used to model log transformed CXCL10 (Equation 10):

$$\log(CXCL10) = a \cdot \log\left(\frac{R}{Baseline_R}\right) + \beta \cdot \log(Baseline_{CXCL10}) + E_0 + \varepsilon \quad (10)$$

Where α and β are the coefficients and E_0 is the intercept reflecting the placebo effect. As both 20060203 and 20070283 studies are placebo-controlled and, since the placebo group did not appear to show any time dependent changes in IFN-γ, the baseline IFN-γ and its' inter-subject variability were estimated using integrated information from the placebo group, pre-dose baseline level in the treatment group and post-dose IFN-γ concentrations when the drug effect was gone. In addition, individual CXCL10 baseline was used to model the CXCL10 response. The CXCL10 concentrations in the placebo group were used to estimate placebo effect designated as E_0 in the linear model of log transformed CXCL10 (Equation 10).

Inter-subject variability of model parameters was described using an exponential error model while the residual unknown variability was assumed to be normally distributed with mean 0 and unknown variance σ^2. Various residual variability models including proportional, additive, and combination of both were tested. In this analysis, the below quantification limit (BQL) concentrations were treated as censored data, and the likelihood of BQL observations was maximized with respect to the model parameters using the Beal's M3 method [19].

Covariate Analysis

Demographic covariates at baseline (sex, race, age and body weight) (Table I) were examined for their influence on the model parameters based on the combined PK/PD dataset with a step-wise method [20]. The empirical Bayes estimates (EBE) were first plotted against covariates, and the correlation coefficients and p-values were calculated. The correlated covariates were then selected for further test. Categorical covariates were incorporated into the model as index variables, whereas continuous covariates were evaluated using power equations after centering on the median. The significant covariates were identified based on the following criteria: 1) a decrease of at least 6.63 in the minimum objective function value (MOFV) at the 0.01 level, approximated by a χ^2-distribution with 1 degree of freedom; 2) improved (as defined below) goodness-of-fit (GOF) plots including predicted *versus* observed concentrations, and weighted residuals *versus* time or predicted concentrations; 3) no significant trend in covariate plots; and 4) decreased standard errors of parameters and between subject variability.

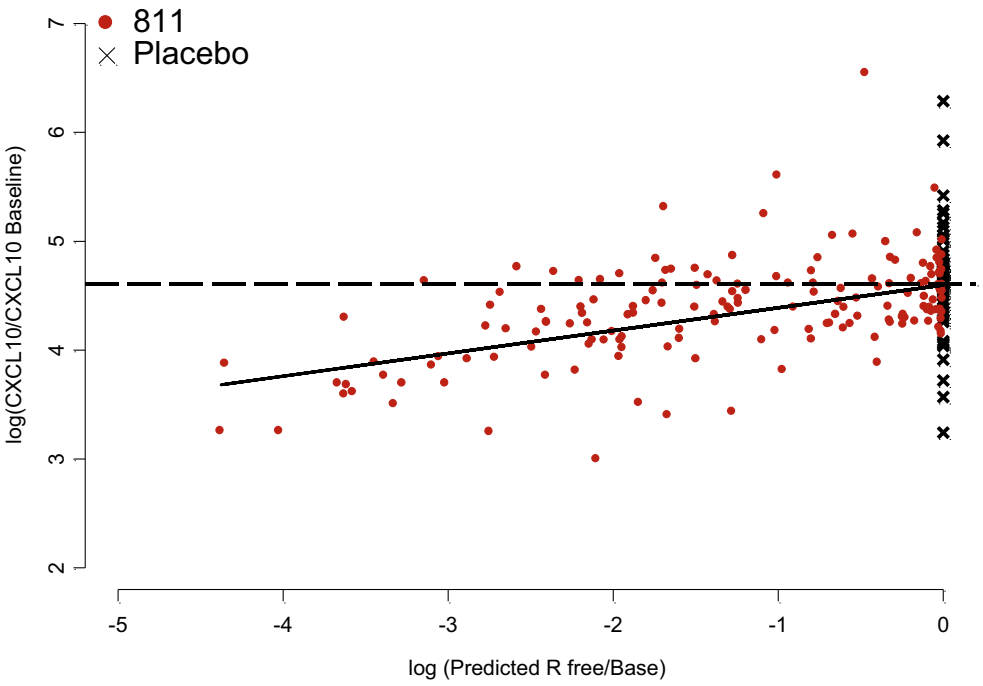

Fig. 2 Relationship between log transformed CXCL10 and log transformed predicted free IFN-γ relative to baseline. The *red dots* (•) represent data from drug treatment group and the cross (x) represent data from placebo group. The *dashed line* represents the expected mean of log transformed percentage of CXCL10 relative to the baseline at time 0 (log (100*CXCL100/baseline) = log (100) = 4.6). The solid *black line* represents the linear regression line of log transformed percentage of CXCL10 relative to the baseline on log transformed predicted free IFN-γ relative to baseline.

Model Evaluation

Model selection was based on improvement in GOF and statistical significance using the MOFV values in NONMEM similarly as described above. When two models were not nested, Akaike Information Criterion (AIC) was used for differentiating the two.

For the final model, visual predictive check (VPC) was used for an internal model evaluation. AMG 811 PK-PD profiles of the same sample size as observed in the analysis dataset were simulated 500 times based on the parameter estimates of the final model, the observed dosing and covariate information for all subjects. The 5, 50 and 95th percentiles of simulated concentrations were plotted with observed values overlaid.

Simulations

To evaluate optimal dosing regimens, simulations for concentrations of AMG 811, total IFN-γ, and CXCL10 after monthly 60, 120 and 180 mg SC doses were performed using the parameter estimates obtained from the final model. The median and 90% prediction interval of the time course of concentrations were also constructed.

Software

The population PK-PD analysis was performed using NONMEM, version VII, Level 2.0 (ICON Development Solutions, Ellicott City, Maryland), a nonlinear mixed-effect modeling software. The stochastic approximation expectation maximization (SAEM) method was used to analyze PK-PD data. For visual predictive check, the simulation profiles was generated by NONMEM. The software R 2.13 was used for dataset assembly, statistical computation, and graphics.

RESULTS

The current dataset included 506 AMG 811 PK concentrations, 460 serum total IFN-γ concentrations, and 284 serum CXCL10 measurements from 54 SLE patients. The percentage of data BQL in AMG 811 PK and CXCL10 was low (<10%) but high (~40%) in total IFN-γ. Compared to excluding BQL data in AMG 811 and CXCL10 analyses, implementing the M3 method to account for these BQL data resulted in almost no change in overall model fit and parameter estimates (data not shown). However, discarding total IFN-γ BQL data resulted in substantial changes (>50%) in parameter estimates such as $Base_{IFN\text{-}\gamma}$ compared to including total IFN-γ BQL in the modeling. Therefore, BQL data of AMG 811 and CXCL10 were excluded and only total IFN-γ BQL data were retained and modeled using the M3 method.

A TMD model with Q_{ss} approximation provided reasonable fit to AMG 811 and total IFN-γ data. The general TMD model was also evaluated [18]. However, implementing the general model resulted in significant increase in the AIC by 174.479 points. As two molecules of IFN-γ can potentially bind to one molecule of AMG 811, a TMD with two binding sites was also explored. However, no improvement was observed which was probably due to the presence of excess AMG 811 concentrations relative to free IFN-γ in the body. Thus, a two compartment Q_{ss} model was selected as structural model. It was noted that during model construction, adding an inter-subject variability on either K_a or F_1 resulted in dramatically prolonged model running time and difficulties in convergence. Therefore, no inter-subject variability was estimated for the two parameters. The population K_{ss} constant is 0.105 nM, about 20 fold larger than K_D obtained from *in-vitro* assay (5 pM). The relationship between log transformed free IFN-γ and log transformed CXCL10 was best described by a linear model with slope and intercept estimated to be 0.197 and -0.3, respectively. An E_{max} model was also evaluated, however, the MOFV increased by 38.511 points and relative standard error (RSE) was large on both EC_{50} and E_{max} parameters suggesting possible over-parameterization of the model. A thorough covariate search based on the PK-PD model identified potential covariate effects of body weight on CL, V_c, Q and V_p, and age on V_c (Fig. 3). Since the range of body weights observed in the current studies is relatively narrow (CV%: ~20%), the exponents were fixed to an allometric scaling constant of 0.75 for CL and Q, and 1 for V_c and V_p. The addition of body weight on CL, V_c, Q and V_p resulted in a reduction of MOFV by 31.174 points. Although weight and age were correlated, age was also identified as a statistically significant covariate on V_c (Fig. 3). The incorporation of age led to the decrease in MOFV by 13.659, and the inter-subject variability (CV%) on V_c was reduced from 75% to 59%. Thus, body weight and age were included in the final model. Based on the estimated body weight effect on CL and V_c, the CL and V_c will increase by approximately 11–14% per each 10 kg of body weight. Based on the estimated age effect on V_c, doubling the age is associated with approximately 91% increase in V_c. Since most patients (94%) enrolled in these studies were female due to SLE prevalence in this population, the effect of sex could not be reliably evaluated on model parameters. In addition, no other covariate effect was observed on PD parameters. The final population PK-PD model and parameter estimates were listed in Table II. The shrinkage values were estimated to be 16.9%, 19.5%, 30.6%, 46.8%, 31.7%, 44.0%, 35.7%, 48.1%, 7.48% and 19.8% for CL, V_c, Q, V_p, D1, k_{deg}, k_{ss}, k_{met}, $Base_{IFN\text{-}\gamma}$ and $Placebo_{CXCL10}$, respectively.

The final goodness-of-fit plots for AMG 811, total IFN-γ, and CXCL10 concentrations are shown in Fig. 4. The plots of population or individual predicted *versus* observed

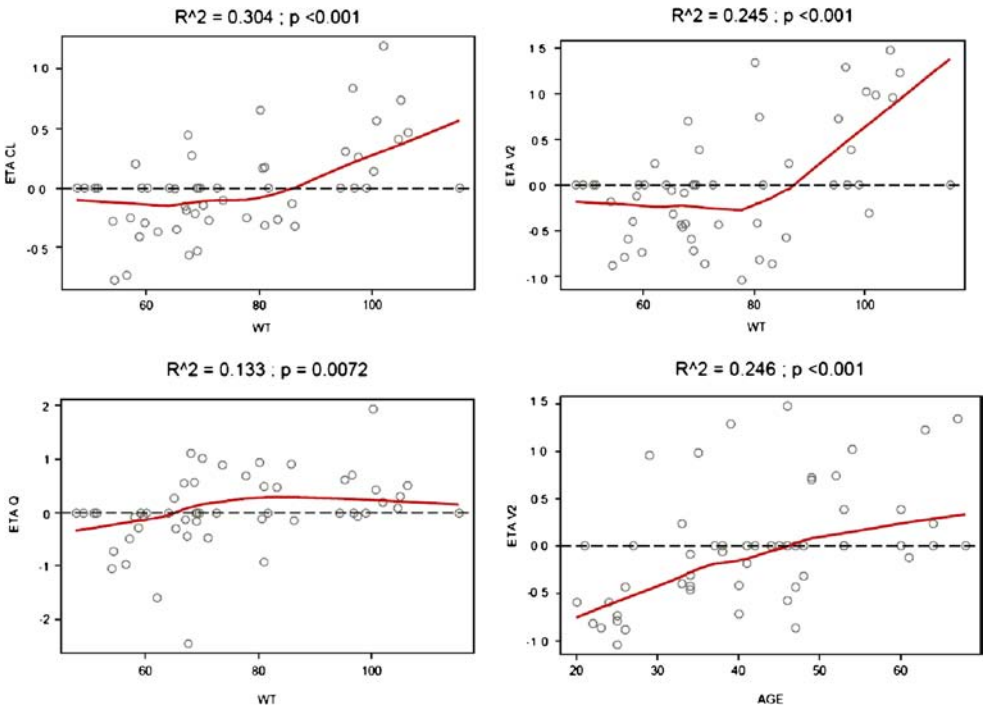

Fig. 3 Correlation between individual EBE and statistically significant covariates. The *red lines* represent loess regression.

concentrations showed that most points fall around the line of identity, which indicated a good agreement between predicted and observed AMG 811, total IFN-γ and CXCL10 concentrations. Although a proportional error model was used in both the PK and CXCL10 model, which put more weight in lower concentrations, a slight under-prediction of AMG 811 and over-prediction of CXCL10 at the lowest concentrations are still noted, which is deemed to have limited relevance.

The visual predictive check shows that simulated AMG 811, total IFN-γ and CXCL10 profiles describe the observed data (Fig. 5) reasonably well, indicating that the final population model captured the variability of data and described time course of AMG 811, total IFN-γ and CXCL10 concentrations adequately. The time course of AMG 811, total IFN-γ and CXCL10 concentrations following 60, 120, and 180 mg QM for a total of 3 doses is displayed in Fig. 6. As shown, drug exposure increased dose proportionally from 60 to 180 mg (Fig. 6(a)). The 120 and 180 mg SC QM dose groups demonstrated higher total IFN-γ increases (Fig. 6(b)) and greater CXCL10 reduction (Fig. 6(c)) compared to the 60 mg SC QM dose. However, we also observed large inter-subject variability and overlap of the 90% prediction interval.

DISCUSSION

A population model was successfully developed to characterize the relationship of serum AMG 811, its target IFN-γ and CXCL10. Consistent with the PK of other monoclonal antibodies, a TMD model with Q_{ss} approximation was suitable to describe the time course of serum AMG 811 concentration. We further simplified the PK model by removing the nonlinear portion caused by interaction with target. The resultant MOFV and inter- and intra-subject variability was almost the same as the original model, which is probably due to the fact that AMG 811 concentrations at given doses are much higher than target (IFN-γ) and the impact of drug-target interaction on AMG 811 PK is negligible. Therefore, in our final PK-PD model, AMG 811 PK is characterized by a two-compartment model with linear elimination.

Describing the absorption process well helps to characterize the overall PK profile. During the model development, high variability in absorption was observed (median t_{max} ranging from 4 to 14 day); furthermore, large molecules do not always follow the typical first order absorption kinetics [21–23]. Therefore, a few empirical models were evaluated to capture the absorption process, including simple first-order absorption (estimating k_a), parallel first-order absorption and sequential zero-order and first-order absorption model. Among these, the last model fit the observed data the best and resulted in a significant decrease in the objection function value (>10) compared to the other absorption models. The sequential zero-order and first-order absorption model has been also used to describe the slow lymphatic absorption process for other biologics, such as darbepoetin [21]. Following the SC administration, AMG 811 has shown slow absorption with absorption half-life ($t_{1/2,abs} = \ln 2/k_a$) estimated to be 3.89 days. This is probably due to the fact that the primary pathway for transport of monoclonal antibody into the blood

Table II Parameter Estimates from the Final Population PK-IFN-γ-CXCL10 Model

Model term	Parameter	Estimate (%RSE)	Inter-Subject variability[a] (%RSE)
$CL = \theta_{CL} \cdot (WT/69.3)^{0.75} \cdot \exp(\eta_{CL})$	θ_{CL} (L/day)	0.176 (6)	36 (15)
$V_c = \theta_{Vc} \cdot (WT/69.3) \cdot (AGE/41.5)^{\theta Vc,AGE} \cdot \exp(\eta_{vc})$	θ_{Vc} (L)	1.48 (35)	48 (19)
	$\theta_{vc,AGE}$	0.93 (37)	
$Q = \theta_{Q} \cdot (WT/69.3)^{0.75} \cdot \exp(\eta_{Q})$	θ_{Q} (L/day)	0.66 (60)	79 (28)
$V_p = \theta_{Vp} \cdot (WT/69.3) \cdot \exp(\eta_{Q} \cdot \theta_{ratio})$	θ_{Vp} (L)	2.12 (7)	47 (12)
	θ_{ratio}	0.35 (12)	
$K_a = \theta_{Ka}$	θ_{Ka} (1/day)	0.178 (22)	
$F_1 = \theta_{F1}$	θ_{F1}	0.44 (70)	
$D_1 = \theta_{D1}$	θ_{D1} (day)	0.12 (16)	110 (77)
$K_{deg} = \theta_{Kdeg} \cdot \exp(\eta_{Kdeg})$	θ_{Kdeg} (1/day)	5.1 (15)	32 (45)
$K_{SS} = \theta_{KSS} \cdot \exp(\eta_{KSS})$	θ_{KSS} (nM)	0.105 (17)	108 (39)
$K_{met} = \theta_{Kmet} \cdot \exp(\eta_{Kmet})$	θ_{Kmet} (1/day)	0.19 (11)	51 (62)
$Base = \theta_{Base} \cdot \exp(\eta_{Base})$	θ_{Base} (nM)	0.00032 (4)	94 (12)
$\log(CXCL10) = Alpha \cdot \log(Rfree/Base\_Rfree) + Beta \cdot \log(Base\_CXCL10) + E_0$			
$Placebo = \theta E_0 + (\eta E_0)$	θE_0	-0.3 (67)	26 (26)
$Alpha = \theta_{Alpha}$	θ_{Alpha}	0.197 (25)	
$Beta = \theta_{Beta}$	θ_{Beta}	0.924 (7)	
$Y_{PK} = F_{PK} \cdot (1 + \varepsilon_1) + \varepsilon_2$	$\sigma_{\_PK\_prop}$ (CV%)[a]	34 (10)	
	$\sigma_{\_PK\_add}$ (SD) (nM)	0.21 (19)	
$Y_{IFN\text{-}\gamma} = F_{IFN\text{-}\gamma} \cdot (1 + \varepsilon_3) + \varepsilon_4$	$\sigma_{\_IFN\text{-}\gamma\_prop}$ (CV%)[a]	62 (2)	
	$\sigma_{\_IFN\text{-}\gamma\_add}$ (SD) (nM)	0.0074 (34)	
$Y_{CXCL10} = F_{CXCL10} \cdot \exp(\varepsilon_5)$	$\sigma_{\_CXCL10\_prop}$ (CV%)[a]	56 (3)	

[a] Inter-individual variability (IIV) and proportional residual error variability were expressed in coefficient variation (CV) as a percentage; additive residual error variability was expressed in standard deviation (SD); RSE% = relative standard error as a percentage

K_a, Absorption rate constant; *F1*, absolute bioavailability; *D1*, duration of zero order kinetics following SC dose administration into depot compartment; *CL*, clearance from central compartment; V_c, V_p, volume of distribution in central and peripheral compartment, respectively; *Q*, inter compartment clearance;. K_{deg}, free IFN-γ degradation rate constant; K_{ss}, Qss rate constant; K_{met}, drug-target elimination rate constant; *Base*, IFN-γ baseline concentration; *Placebo*, CXCL10 placebo effect E_0; *Alpha*, the slope of log (Rfree/base_Rfree); *Beta*, the slope of log (Base_CXCL10); $\sigma_{\_PK\_prop}$, $\sigma_{\_IFN\text{-}\gamma\_prop}$ and $\sigma_{\_CXCL10\_prop}$ = approximate proportional residual error expressed in CV% for PK, IFN-γ and CXCL10, respectively; $\sigma_{\_PK\_add}$ and $\sigma_{\_IFN\text{-}\gamma\_add}$ = approximate additive residual error expressed in SD for PK and IFN-γ, respectively

was through lymphatic vessels and the flow rate of the lymphatic system was relatively slow.

The bioavailability of AMG 811 was estimated to be 44% [36%, 52%] (mean [95% confidence interval]) which was slightly lower than other monoclonal antibodies such as denosumab (*F*=64%) [24], and efalizumab (*F*=56%) [25]. Multiple factors could impact the SC bioavailability such as pre-systemic catabolism and rate of recycling of monoclonal antibody by interacting with the neonatal Fc receptor (FcRn) [26]. In addition, studies have shown that IFN-γ production is overexpressed by lymph node cells in autoimmune (MRL/1, MRL/n) mice [27]. Lymphoid IFN-γ mRNA is also upregulated in autoimmune MRL-Fas (lpr) mice with lupus nephritis [28]. Thus, the potential binding of AMG 811 to IFN-γ in lymphatic tissue may contribute to the lower bioavailability of AMG 811 compared to other monoclonal antibodies. Nevertheless, even if IFN-γ may be overexpressed in lymphatic tissues, the observed antibody ligand ratio in the current study suggested very low concentrations of free IFN-γ in circulation system.

The population clearance was estimated to be 0.176 L/day for the median 69.3 kg subject following IV administration which was within the range of CL of 0.066-0.535 L/day reported in other human monoclonal antibodies of the same isotype [29]. In addition, the CL of AMG 811 was found to be close to the CL of endogenous IgG (0.21 L/day), which in turn suggested that target mediated disposition of AMG 811 could be negligible at the concentrations evaluated in current analysis. Compared to anti- IFN-γ antibody fontolizumab (CL= 0.16~0.18 mL/hr/kg) [16], AMG 811 has shown slower CL (0.106 mL/hr/kg), which could be due to different affinities of these two molecules to broadly expressed receptors such as FcRn or Fcγ receptors. The central and peripheral volumes of distribution of AMG 811 are 1.48 and 2.12 L, respectively, with the volume of distribution at steady state (V_{ss}) [calculated as $V_c + V_p$] estimated to be 3.6 L. Compared to the V_{ss}

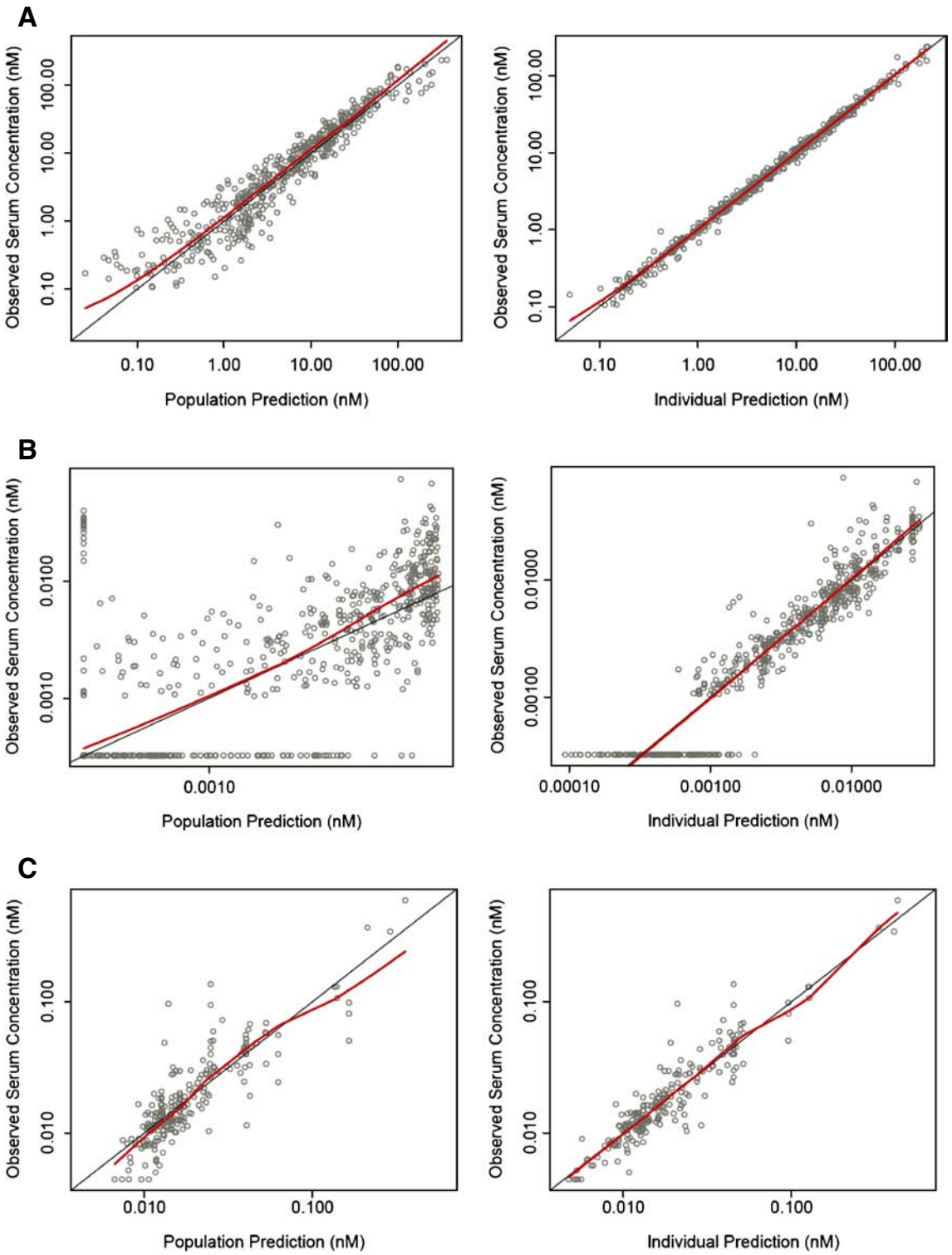

Fig. 4 Goodness-of-fit plots for the final PK/PD model. Plot of individual (*right*) and population predicted (*left*) *versus* observed AMG 811 PK (**a**), total IFN-γ (**b**), and CXCL10 (**c**) concentrations. The *black lines* represent the line of identity and the *red lines* represent loess regression line of data points.

observed in efalizumab (V_{ss}=6.76 L) [25], panitumumab (V_{ss}=6.54 L) [30], fontolizumab (V_{ss}=5.8~6.6 L assuming 70 kg body weight) [16] and tocilizumab (V_{ss}=6.4 L) [31], AMG 811 exhibits a relatively low volume of distribution. On the other hand, AMG 811 has a similar V_{ss} as denosumab (V_{ss}=3.85 L) [24]. Due to its relatively large size, the distribution of antibodies is usually limited to the extracellular or intravascular space [32]. The estimated V of

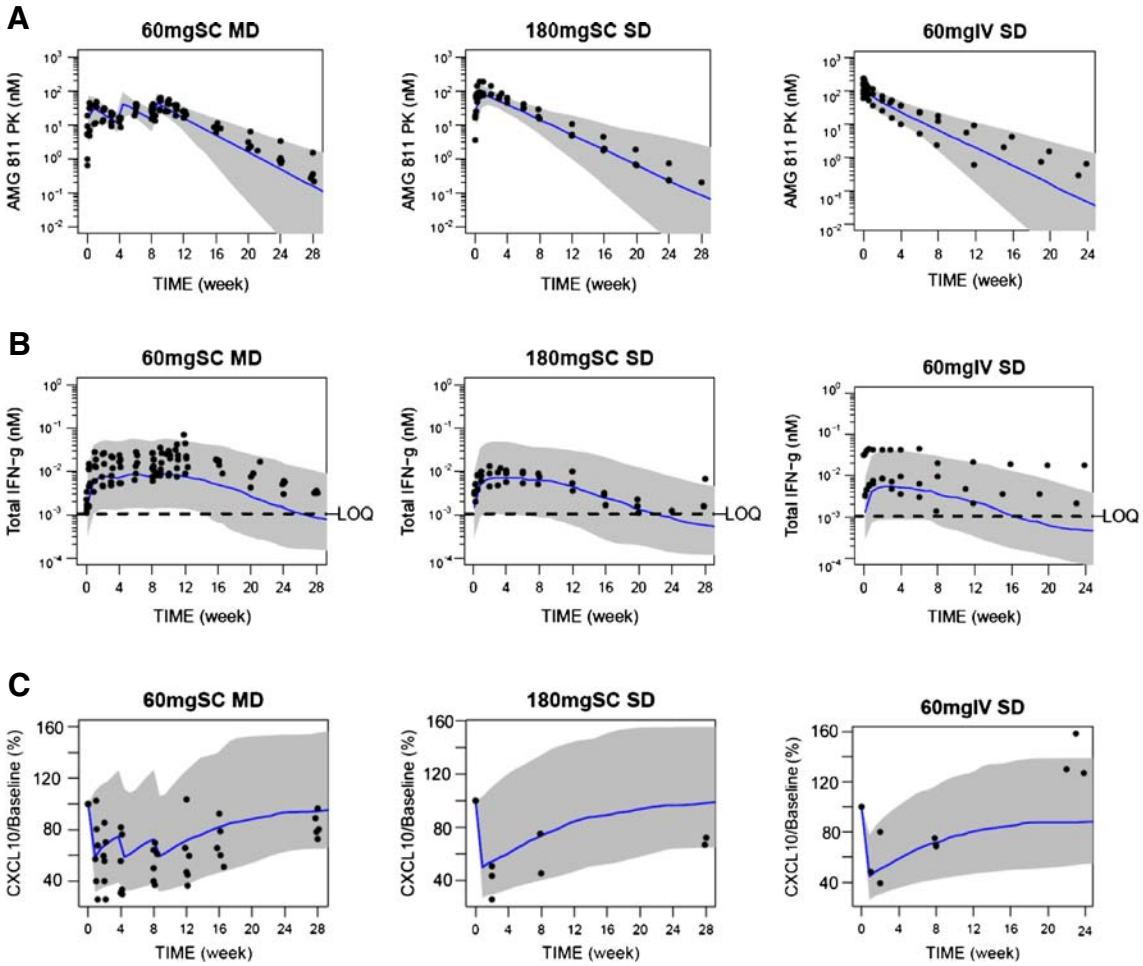

Fig. 5 Visual predictive check (VPC) plots stratified by dosing regimen. 500 datasets were simulated using the final PK-PD model parameter estimates. The observed (•) data were overlaid with predicted median (—) and 90% prediction interval (*shaded grey area*) for AMG 811 PK (**a**), total IFN-γ (**b**) and CXCL10 (**c**).

AMG 811 was close to the plasma volume indicating the limited extravascular distribution of AMG 811. It is noteworthy that the vast majority (>90%) of subjects enrolled in the AMG 811 Phase 1 studies were female, as would be expected from a SLE population. On average, total body water, extracellular or intracellular water, total blood volume and plasma volume are greater in male than female. Therefore, the high percentage of female patients in this study may have contributed to the smaller volume of distribution compared to a more gender balanced study conducted for the other antibodies.

Body weight and age were identified as statistically significant covariates on PK parameters. Although previous studies suggested elevated IFN-γ levels in heavier subjects [33] and increased serum CXCL10 levels with advancing age [34], no significant correlation was observed between weight/age and baseline IFN-γ and CXCL10 with the current data. This is likely due to the relatively small sample size. Besides, age and weight were correlated. Thus, the impact of age on AMG 811 PK and PD should be reassessed when additional clinical data become available. Since the inter-subject variability was relatively large, and concentrations after therapeutic doses (>60 mg SC QM) were approaching the plateau of the exposure-response relationship based on the simulations of total IFN-γ and CXCL10, dose adjustment based on body weight and age may not be necessary.

In human, there is evidence that IFN-γ is elevated in SLE patients [8–12]. However, even in SLE patients, endogenous IFN-γ levels are quite low and are often close to the LLOQ. Thus, the ELISA assay developed directly measured serum total IFN-γ levels with a LLOQ of 50 pg/mL. Due to very low free IFN-γ concentrations present in the circulation system, the majority of measured IFN-γ levels at pretreatment and placebo group are BQL. Studies have shown that ignoring BQL data was associated with substantial bias in parameter estimates and thus, treating BQL data as censored observations (M3) is considered as the best option for handling BQL [19, 35]. After incorporating the M3 method in the model, the estimated IFN-γ baseline was 0.32 pM (~15 pg/mL) consistent with at least one report [36].

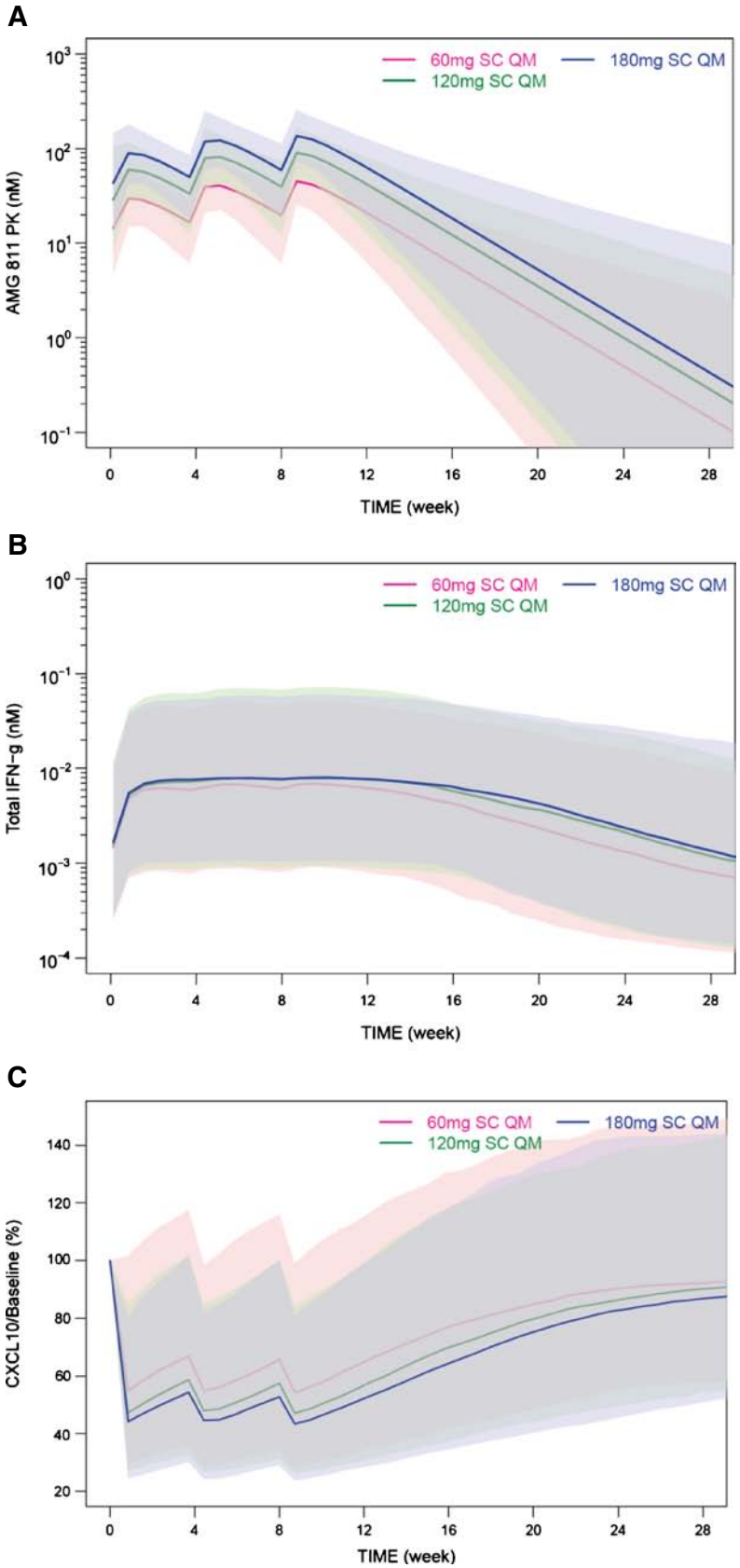

Fig. 6 Predicted Serum AMG 811 (**a**), total IFN-γ (**b**) and CXCL10 (**c**) concentration-time course in SLE subjects with 3-month treatment of 60, 120, 180 mg Q4W for a total of 3 doses. The *solid lines* represent population predicted profile and shaded areas represent 90% prediction interval.

The availability of total IFN-γ information enables a better understanding of the AMG 811 mechanism of action. Total IFN-γ is characterized by the TMD-Q_{SS} model. The TMD-Q_{SS} model is widely used for compounds showing non-linear PK. Our PK-PD exercise demonstrated that TMD-Q_{SS} model is also suitable to fit target concentration even when the drug exhibited linear PK. The estimated population degradation rate constant for free IFN-γ (k_{deg}) was much higher than the estimated elimination rate constant for drug-target complex (k_{met}), indicating that drug-target complex could be eliminated much slower than the normally rapid clearance of free IFN-γ. This is consistent with the observation that administration of AMG 811 led to a rapid increase in total IFN-γ probably due to the accumulation of drug-target complex. A previous simulation study [37] also showed that R_{tot} increases if k_{met} (refer to k_{int} in the reference paper) is less than k_{deg}. The estimated K_{ss} is much higher than K_d probably due to several factors. One of them is the fact that K_{ss} is the sum of K_d and K_{met}/K_{on}, and consequently K_{ss} should be higher than K_d. In addition, the conditions of a simple *in vitro* system used to determine K_d do not normally represent the complex *in vivo* system where K_{ss} is determined. A recent study on theoretical consideration of TMDD models [38] has included more discussion on this discrepancy of the modeling resulted K_{ss} with *in vitro* K_d. The estimated k_{deg} of endogenous IFN-γ is 5.1 day^{-1} and the derived half-life of IFN-γ is 3.26 hours ($t_{1/2}=0.693/k_{deg}$) which is consistent with the reported half-life of 2 ~ 3 hours for recombinant IFN-γ [39]. However, large variation is also noted for the half-life of IFN-γ reported from literature which ranges from $t_{1/2}$ of ~30 min [40] to 6.8 hours [41]. This discrepancy may be explained by different drug formulation, assay and/or biological matrix used by different researchers.

CXCL10 is a chemokine secreted by several cell types including monocytes, endothelial cells, and fibroblasts. Mechanistically, IFN-γ induces CXCL10 gene expression and results in CXCL10 protein production [42]. Other cytokines, such as IFN-α/β and TNF, and viral glycoproteins can also induce CXCL10 production *in vitro*. With a TMD model, we were able to derive the equation for free ligand based on the AMG 811 PK and total ligand information (Equation 9) and simultaneously modeled AMG 811 concentrations, total IFN-γ and CXCL10 concentrations by linking derived free IFN-γ with measured CXCL10. Several studies have shown that serum CXCL10 are elevated in SLE, and its expression correlates with disease activity and clinical manifestations in SLE [11, 43, 44]. Compared to standard laboratory test such as erythrocyte sedimentation rate, complement factor levels and anti-double-stranded DNA antibodies, serum CXCL10 levels appears to be a better predictor of future SLE disease flares [14]. In a validation study, serum CXCL10 levels were found to rise at the time of SLE flare and fall as disease remitted [14]. Recent study also confirmed that CXCL10 levels were significantly reduced in treated compared to untreated SLE patients [45]. Although these findings suggest that CXCL10 reduction is an important biomarker for therapeutic efficacy in SLE patients, it has not been yet qualified as a surrogate marker. So far, there is no evidence that there is a specific target reduction of CXCL10, and therefore, establishing the dose-biomarker response relationship will inform the testing of doses of AMG 811 that maximally reduce CXCL10 and corresponding assessment of clinical impact. This working hypothesis needs to be confirmed in upcoming clinical trials. The simulations across the doses of monthly 60, 120 and 180 mg SC indicated a clear dose-response relationship with CXCL10. The greatest reduction of CXCL10 was achieved at the highest dose tested (180 mg). Monthly dosing appeared to be sufficient to maintain the sustained CXCL10 suppression during the entire dosing interval. Compared to the highest multiple dose (60 mg) evaluated in SLE subjects thus far, multiple monthly 120 or 180 mg dosing may provide additional benefit on CXCL10 suppression.

The goodness-of-fit and visual predictive check shows that the current model describes the observed AMG 811, total IFN-γ and CXCL10 profiles reasonably well although a slight under-prediction of AMG 811 and over-prediction of CXCL10 at the lowest concentrations are noted in Fig. 4. The under-prediction of AMG 811 concentrations may be because these lowest concentrations are around the assay limit of quantification. More PK data at low doses (eg. 2 mg) may help model these lowest concentrations. However, our PK/PD modeling and simulation suggested that the therapeutic dose of AMG 811 would be greater than 60 mg. The under-prediction of AMG 811 at lowest concentrations poses low risk in applying current model to help future study design. The over-prediction of CXCL10 concentrations at the lowest concentrations may be due to the large variability in the observed CXCL10 concentrations and the lack of higher dose data (i.e. >60 mg multiple dose) to better characterize CXCL10 maximum suppression (i.e. lowest CXCL10 concentrations). Simulation results suggested that a higher dose (120 or 180 mg multiple dose) will provide additional benefit on CXCL10 suppression and will help to better understand the shape of the CXCL10 model.

CONCLUSION

In summary, a mechanism-based TMD model coupled with a linear model to link log transformed estimated free IFN-γ and log-transformed CXCL10 was developed to simultaneously fit and describe serum AMG 811, its target IFN-γ and CXCL10 concentration-time course profiles. To our knowledge, this is the first time that the interaction between drug, IFN-γ and

CXCL10 has been quantitatively characterized. These results may be used to guide dose selection for future AMG 811 studies and provide scientific rationale for dose optimization.

ACKNOWLEDGMENTS AND DISCLOSURES

The authors thank all the patients, the investigators, and their medical, nursing, and laboratory staff who participated in the clinical studies included in the present analysis. These studies were sponsored by Amgen Inc., which was involved in the study design, data collection, analysis, interpretation, writing the manuscript, and the decision to submit the manuscript for publication. Ping Chen, Thuy Vu, Adimoolam Narayanan, Winnie Sohn, Jin Wang, Michael Boedigheimer, Andrew Welcher, Barbara Sullivan, David Martin, and Juan Jose Perez Ruixo are employees of Amgen Inc. and own stock in Amgen Inc. at the time this analysis was conducted. Peiming Ma is a former employee of Amgen Inc. The authors have no other conflict of interest to declare.

REFERENCES

1. Finkelman FD, Katona IM, Mosmann TR, Coffman RL. IFN-gamma regulates the isotypes of Ig secreted during in vivo humoral immune responses. J Immunol. 1988;140:1022–7.
2. Boehm U, Klamp T, Groot M, Howard JC. Cellular responses to interferon-gamma. Annu Rev Immunol. 1997;15:749–95.
3. Rauch I, Muller M, Decker T. The regulation of inflammation by interferons and their STATs. JAKSTAT. 2013;2:e23820.
4. Theofilopoulos AN, Koundouris S, Kono DH, Lawson BR. The role of IFN-gamma in systemic lupus erythematosus: a challenge to the Th1/Th2 paradigm in autoimmunity. Arthritis Res. 2001;3:136–41.
5. Theofilopoulosand AN, Kono DH. Genetics of systemic autoimmunity and glomerulonephritis in mouse models of lupus. Nephrology, dialysis, transplantation : official publication of the European Dialysis and Transplant Association - European Renal Association. 16 Suppl 6:65–67 (2001).
6. Lee JY, Goldman D, Piliero LM, Petri M, Sullivan KE. Interferon-gamma polymorphisms in systemic lupus erythematosus. Genes and immun. 2001;2:254–7.
7. Baechler EC, Batliwalla FM, Karypis G, Gaffney PM, Ortmann WA, Espe KJ, *et al.* Interferon-inducible gene expression signature in peripheral blood cells of patients with severe lupus. Proc Natl Acad Sci U S A. 2003;100:2610–5.
8. Funauchi M, Sugishima H, Minoda M, Horiuchi A. Serum level of interferon-gamma in autoimmune diseases. Tohoku J Exp Med. 1991;164:259–67.
9. Yokoyama H, Takabatake T, Takaeda M, Wada T, Naito T, Ikeda K, *et al.* Up-regulated MHC-class II expression and gamma-IFN and soluble IL-2R in lupus nephritis. Kidney Int. 1992;42:755–63.
10. al-Janadi M, al-Balla S, al-Dalaan A, Raziuddin S. Cytokine profile in systemic lupus erythematosus, rheumatoid arthritis, and other rheumatic diseases. J Clin Immunol. 1993;13:58–67.
11. Narumi S, Takeuchi T, Kobayashi Y, Konishi K. Serum levels of ifn-inducible PROTEIN-10 relating to the activity of systemic lupus erythematosus. Cytokine. 2000;12:1561–5.
12. Samsonov MY, Tilz GP, Egorova O, Reibnegger G, Balabanova RM, Nassonov EL, *et al.* Serum soluble markers of immune activation and disease activity in systemic lupus erythematosus. Lupus. 1995;4:29–32.
13. Hammon M, Herrmann M, Bleiziffer O, Pryymachuk G, Andreoli L, Munoz LE, *et al.* Role of guanylate binding protein-1 in vascular defects associated with chronic inflammatory diseases. J Cell Mol Med. 2011;15:1582–92.
14. Bauer JW, Petri M, Batliwalla FM, Koeuth T, Wilson J, Slattery C, *et al.* Interferon-regulated chemokines as biomarkers of systemic lupus erythematosus disease activity: a validation study. Arthritis Rheum. 2009;60:3098–107.
15. Martin DA, Boedigheimer M, Amoura Z, Kivitz A, Buyon J, Sanchez-Guerrero J, *et al.* AMG 811 (anti-IFN-gamma) treatment leads to a reduction in the whole blood IFN-signature and serum CXCL10 in Subjects with Systemic Lupus Erythematosus: Results of two Phase I Studies., *the 77th Annual ACR meeting*, San Diego, CA 2013.
16. Hommes DW, Mikhajlova TL, Stoinov S, Stimac D, Vucelic B, Lonovics J, *et al.* Fontolizumab, a humanised anti-interferon gamma antibody, demonstrates safety and clinical activity in patients with moderate to severe Crohn's disease. Gut. 2006;55:1131–7.
17. Magerand DE, Jusko WJ. General pharmacokinetic model for drugs exhibiting target-mediated drug disposition. J Pharmacokinet Pharmacodyn. 2001;28:507–32.
18. Gibiansky L, Gibiansky E, Kakkar T, Ma P. Approximations of the target-mediated drug disposition model and identifiability of model parameters. J Pharmacokinet Pharmacodyn. 2008;35:573–91.
19. Ahn JE, Karlsson MO, Dunne A, Ludden TM. Likelihood based approaches to handling data below the quantification limit using NONMEM VI. J Pharmacokinet Pharmacodyn. 2008;35:401–21.
20. Mandema JW, Verotta D, Sheiner LB. Building population pharmacokinetic–pharmacodynamic models. I. Models for covariate effects. J Pharmacokinet Biopharm. 1992;20:511–28.
21. Doshi S, Chow A, Perez Ruixo JJ. Exposure-response modeling of darbepoetin alfa in anemic patients with chronic kidney disease not receiving dialysis. J Clin Pharmacol. 2010;50:75S–90S.
22. Radwanski E, Chakraborty A, Van Wart S, Huhn RD, Cutler DL, Affrime MB, *et al.* Pharmacokinetics and leukocyte responses of recombinant human interleukin-10. Pharm Res. 1998;15:1895–901.
23. Richter WF, Bhansali SG, Morris ME. Mechanistic determinants of biotherapeutics absorption following SC administration. AAPS J. 2012;14:559–70.
24. Sutjandra L, Rodriguez RD, Doshi S, Ma M, Peterson MC, Jang GR, *et al.* Population pharmacokinetic meta-analysis of denosumab in healthy subjects and postmenopausal women with osteopenia or osteoporosis. Clin Pharmacokinet. 2011;50:793–807.
25. Ng CM, Joshi A, Dedrick RL, Garovoy MR, Bauer RJ. Pharmacokinetic-pharmacodynamic-efficacy analysis of efalizumab in patients with moderate to severe psoriasis. Pharm Res. 2005;22:1088–100.
26. Wang W, Wang EQ, Balthasar JP. Monoclonal antibody pharmacokinetics and pharmacodynamics. Clin Pharmacol Ther. 2008;84:548–58.
27. Manolios N, Schrieber L, Nelson M, Geczy CL. Enhanced interferon-gamma (IFN) production by lymph node cells from autoimmune (MRL/1, MRL/n) mice. Clin Exp Immunol. 1989;76:301–6.
28. Fanand X, Wuthrich RP. Upregulation of lymphoid and renal interferon-gamma mRNA in autoimmune MRL-Fas (lpr) mice with lupus nephritis. Inflammation. 1997;21:105–12.
29. Dirksand NL, Meibohm B. Population pharmacokinetics of therapeutic monoclonal antibodies. Clin Pharmacokinet. 2010;49:633–59.
30. Ma P, Yang BB, Wang YM, Peterson M, Narayanan A, Sutjandra L, *et al.* Population pharmacokinetic analysis of panitumumab in

patients with advanced solid tumors. J Clin Pharmacol. 2009;49: 1142–56.
31. Frey N, Grange S, Woodworth T. Population pharmacokinetic analysis of tocilizumab in patients with rheumatoid arthritis. J Clin Pharmacol. 2010;50:754–66.
32. Tang L, Persky AM, Hochhaus G, Meibohm B. Pharmacokinetic aspects of biotechnology products. J Pharm Sci. 2004;93:2184–204.
33. Utsal L, Tillmann V, Zilmer M, Maestu J, Purge P, Jurimae J, *et al.* Elevated serum IL-6, IL-8, MCP-1, CRP, and IFN-gamma levels in 10- to 11-year-old boys with increased BMI. Horm res in paediatr. 2012;78:31–9.
34. Shurin GV, Yurkovetsky ZR, Chatta GS, Tourkova IL, Shurin MR, Lokshin AE. Dynamic alteration of soluble serum biomarkers in healthy aging. Cytokine. 2007;39:123–9.
35. Bergstrandand M, Karlsson MO. Handling data below the limit of quantification in mixed effect models. AAPS J. 2009;11:371–80.
36. Tokano Y, Morimoto S, Kaneko H, Amano H, Nozawa K, Takasaki Y, *et al.* Levels of IL-12 in the sera of patients with systemic lupus erythematosus (SLE)–relation to Th1- and Th2-derived cytokines. Clin Exp Immunol. 1999;116:169–73.
37. Yan X, Mager DE, Krzyzanski W. Selection between Michaelis-Menten and target-mediated drug disposition pharmacokinetic models. J Pharmacokinet Pharmacodyn. 2010;37:25–47.
38. Ma P. Theoretical considerations of target-mediated drug disposition models: simplifications and approximations. Pharm Res. 2012;29: 866–82.
39. Thompson JA, Lee DJ, Cox WW, Lindgren CG, Collins C, Neraas KA, *et al.* Recombinant interleukin 2 toxicity, pharmacokinetics, and immunomodulatory effects in a phase I trial. Cancer Res. 1987;47:4202–7.
40. Gutterman JU, Rosenblum MG, Rios A, Fritsche HA, Quesada JR. Pharmacokinetic study of partially pure gamma-interferon in cancer patients. Cancer Res. 1984;44:4164–71.
41. Turner PK, Houghton JA, Petak I, Tillman DM, Douglas L, Schwartzberg L, *et al.* Interferon-gamma pharmacokinetics and pharmacodynamics in patients with colorectal cancer. Cancer Chemother Pharmacol. 2004;53:253–60.
42. Luster AD, Unkeless JC, Ravetch JV. Gamma-interferon transcriptionally regulates an early-response gene containing homology to platelet proteins. Nature. 1985;315:672–6.
43. Kong KO, Tan AW, Thong BY, Lian TY, Cheng YK, Teh CL, *et al.* Enhanced expression of interferon-inducible protein-10 correlates with disease activity and clinical manifestations in systemic lupus erythematosus. Clin Exp Immunol. 2009;156:134–40.
44. Rose T, Grutzkau A, Hirseland H, Huscher D, Dahnrich C, Dzionek A, *et al.* IFNalpha and its response proteins, IP-10 and SIGLEC-1, are biomarkers of disease activity in systemic lupus erythematosus. Ann Rheum Dis. 2013;72:1639–45.
45. Dominguez-Gutierrez PR, Ceribelli A, Satoh M, Sobel ES, Reeves WH, Chan EK. Reduced levels of CCL2 and CXCL10 in systemic lupus erythematosus patients under treatment with prednisone, mycophenolate mofetil, or hydroxychloroquine, except in a high STAT1 subset. Arthritis res & ther. 2014;16:R23.